ESTIMATION OF SPATIALLY AND TIME VARYING HEAT FLUX VIA MARKOV CHAIN MONTE CARLO METHOD AND INTEGRAL TRANSFORMS

Marques Fredman Mescolin, mmescolin@iff.edu.br[1,2]
Luiz Alberto da Silva Abreu, luiz.abreu@iprj.uerj.br[1]
Diego Campos Knupp, diegoknupp@iprj.uerj.br[1]
Antônio José da Silva Neto, ajsneto@iprj.uerj.br[1]
Mech. Eng. Dept. – Polytechnic Institute, Rio de Janeiro State University, UERJ, Nova Friburgo, Brazil[1]
Fluminense Federal Institute of Education Science and Technology, IFF, Macaé, Brazil[2]

Abstract. *This work addresses the inverse heat conduction problem to estimate a spatially and time varying heat flux imposed to a thermally thin plate within the Bayesian framework, employing the Markov Chain Monte Carlo method. In order to allow for the computer intensive task required by the inverse problem solution, the physical problem is modelled thorough a lumped formulation across the sample thickness, and the resulting differential equation is solved by means of the hybrid analytical-numerical methodology known as the Generalized Integral Transform Technique. The inverse problem solution considers simulated transient measurements on the plate surface, as obtainable, for instance, through an infrared thermography system. Different Markov Random Fields priors are combined and analyzed for the estimation of the heat flux with variation in time and space: a total variation density and a Gaussian smoothness density. We also propose a combination of both, using a total variation prior for the space regularizations and a Gaussian smoothness variation for time regularization. The preliminary results obtained indicate the feasibility of the proposed approach, specially the combination of the total varation and Gaussian smoothness priors, which yielded the best results.*

Keywords*: Inverse problems, Boundary flux estimation, Bayesian inference, Integral transforms, Hybrid methods*

1. INTRODUCTION

The inverse heat conduction problem of estimating boundary heat fluxes or internal heat sources has caught the attention of many researchers along the last three decades, at least, mainly driven by the numerous practical applications in different fields: fatigue (Doudard et al, 2010), microreactors (Pradere et al, 2006), detection of tumors (Mital and Scott, 2006), scanning transparent objects (Eren et al, 2009) and detection of objects with occurrence of corrosion (Marinetti and Valivov, 2010) as well as many other applications. Without the pretension of performing an extensive literature review within this topic, we may cite some early works for the simultaneous estimation of location and time variation of strength in plane heat sources employing the conjugate gradient method in a plate (Silva Neto and Ozisik, 1993; Silva Neto and Ozisik, 1994) and cylindrical rods (Su and Silva Neto, 2001). Later, the development of non-intrusive temperature measurement systems with high space resolution and acquisition frequency, such as infrared thermography systems, brought a renewed interest to these works, for example aiming at the identification of multiple heat sources (Le Niliot and Lefèvre, 2001). More recently, with the propagation in engineering applications of efficient sampling methods, such as the Markov Chain Monte Carlo (MCMC) within the Bayesian inference approach (Kaipio and Sommersalo, 2004), more involved problems could be dealt, such as the space and/or time variable boundary heat flux estimation employing prior models derived from the Markov Random Fields theory (Wang and Zabaras, 2004; Orlande et al , 2014).

Regarding very recent technological applications, the continuous demands for miniaturization of electronic equipment and consequent increase in heat dissipation needs led to intense research on the thermal management of those devices, with special attention to the remediation of hot spots (Hetsroni et al, 2001; Bar-Cohen and Wang, 2012). In this case, the accurate reconstruction of the boundary heat flux in electronic chip packaging, including the space and time variation of strength, employing external non-intrusive measurements, becomes of paramount relevance (Chen and Hsu, 2007; Chen and Yang, 2007; Cheng and Chen, 2010). In this context, this article deals with the inverse heat conduction problem to estimate a spatially and time varying heat flux within the Bayesian framework employing the Markov Chain Monte Carlo method. In order to allow for the computer intensive task required by the inverse problem solution, the physical problem consisting of a thermally thin plate with imposed spatially and time varying heat flux is modelled thorough a lumped formulation across the sample thickness (Cotta and Mikhailov, 1997), and the resulting differential equation is solved by means of the hybrid analytical-numerical methodology known as the Generalized Integral Transform Technique (GITT) (Cotta, 1993). The inverse problem solution considers simulated transient measurements on the plate surface, as obtainable, for instance, through an infrared thermography system. Different Markov Random Fields priors are combined and analyzed for the estimation of the heat flux with variation in time and space: a total variation density and a Gaussian smoothness density. We also propose a combination of both, using a total variation prior for the space regularizations and a Gaussian smoothness prior for time regularization.

2. FORWARD PROBLEM

Consider a thin plate with a prescribed heat flux $q(x,y,t)$ at $z=0$, and exchanging heat with the environment at the opposite face, $z=L_z$, as schematically shown in Figure 1. The heat conduction equations modeling this problem, including initial and boundary conditions neglecting losses through the borders, are given by:

$$\rho c_p \frac{\partial T(\mathbf{x},t)}{\partial t} = k\nabla^2 T(\mathbf{x},t), \quad \mathbf{x}\in V, \quad t>0 \tag{1a}$$

$$-k\frac{\partial T(\mathbf{x},t)}{\partial \mathbf{n}} = q(x,y,t), \quad z=0; \quad k\frac{\partial T(\mathbf{x},t)}{\partial \mathbf{n}} = h\left[T_\infty - T(\mathbf{x},t)\right], \quad z=L_z \tag{1b,c}$$

$$\frac{\partial T(\mathbf{x},t)}{\partial \mathbf{n}} = 0, \quad x=0,\ x=L_x,\ y=0,\ y=L_y \tag{1d}$$

$$T(\mathbf{x},0) = T_\infty \tag{1e}$$

If one further assumes that the flux is constant through the lateral direction of the plate, y, i.e. $q(x,y,t)\equiv q(x,t)$, the diffusion term on the direction y can be neglected. Moreover, if the Biot number calculated over the direction z is sufficiently low, it is reasonable to consider a lumped formulation (Cotta and Mikhailov, 1997) across this direction, as further detailed in (Knupp et al, 2012). With these assumptions, the following simplified mathematical model can be employed:

$$\rho c_p \frac{\partial T(x,t)}{\partial t} = k\frac{\partial^2 T(x,t)}{\partial x^2} + \frac{q(x,t)}{L_z} - \frac{h}{L_z}(T(x,t)-T_\infty), \quad x\in[0,L_x], \quad t>0 \tag{2a}$$

$$\left.\frac{\partial T(x,t)}{\partial x}\right|_{x=0} = \left.\frac{\partial T(x,t)}{\partial x}\right|_{x=L_x} = 0 \tag{2b}$$

$$T(x,0) = T_\infty \tag{2c}$$

where ρ is the plate's specific mass, c_p its specific heat, k its thermal conductivity, T_∞ is the room temperature and the h is the heat transfer coefficient.

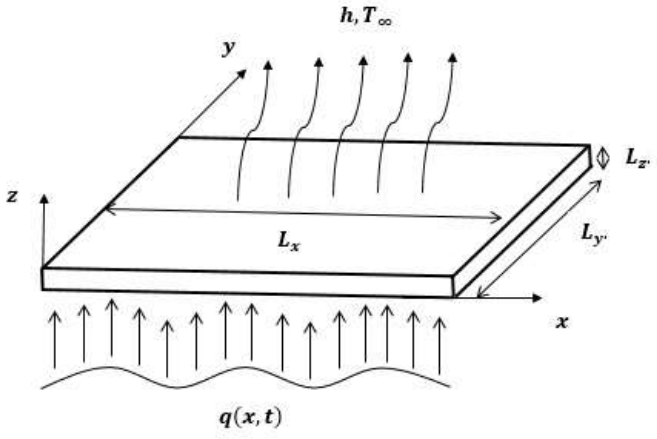

Figure 1. Schematic of the physical problem.

In order to solve the problem given by Eqs. (2a-c) we first propose a filter to reduce the importance of the equation source term, in the form:

$$T(x,t) = T_\infty + T^*(x,t) \tag{3}$$

yielding:

$$\rho c_p \frac{\partial T^*(x,t)}{\partial t} = k\frac{\partial^2 T^*(x,t)}{\partial x^2} - \frac{h}{L_z}T^*(x,t) + \frac{q(x,t)}{L_z}, \quad x \in [0, L_x], \quad t > 0 \tag{4a}$$

$$\left.\frac{\partial T^*(x,t)}{\partial x}\right|_{x=0} = \left.\frac{\partial T^*(x,t)}{\partial x}\right|_{x=L_x} = 0 \tag{4b}$$

$$T^*(x,0) = 0 \tag{4c}$$

Following the formal solution procedure via the Generalized Integral Transform Technique (Cotta, 1993), the following eigenproblem is proposed, obtained from the direct application of separation of variables to the homogeneous version of the problem given by Eqs. (4a-c):

$$k\frac{d^2\psi_i(x)}{dx^2} + \left(\rho c_p \mu_i^2 - \frac{h}{L_z}\right)\psi_i(x) = 0, \quad x \in [0, L_x] \tag{5a}$$

$$\left.\frac{\partial \psi_i(x)}{\partial x}\right|_{x=0} = \left.\frac{\partial \psi_i(x)}{\partial x}\right|_{x=L_x} = 0 \tag{5b}$$

which allows for explicit exact solution for the eigenfunctions $\psi_i(x)$ and the corresponding eigenvalues μ_i^2. Then, based on the orthogonality property of the eigenfunctions, the following transform-inverse pair can be stated:

$$\text{Transform:} \quad \bar{T}_i^*(t) = \int_0^{L_x} \rho c_p T^*(x,t)\tilde{\psi}_i(x)dx \tag{6a}$$

$$\text{Inverse:} \quad T^*(x,t) = \sum_{i=1}^{\infty} \tilde{\psi}_i(x)\bar{T}_i^*(t) \tag{6b}$$

where $\tilde{\psi}_i(x)$ are the normalized eigenfunctions, calculated as:

$$\tilde{\psi}_i(x) = \frac{\psi_i(x)}{N_i^{1/2}}, \text{ with } N_i = \int_0^{L_x} \rho c_p \left[\tilde{\psi}_i(x)\right]^2 dx \tag{7a,b}$$

Operating on Eq. (4a) with $\int_0^{L_x} \tilde{\psi}_i(x)(\cdot)\,dx$, making use of the boundary conditions in Eqs. (4b) and (5b), and operating on the initial condition, Eq. (4c), with $\int_0^{L_x} \rho c_p \tilde{\psi}_i(x)(\cdot)\,dx$ yields the following transformed problem:

$$\frac{d\bar{T}_i^*(t)}{dt} + \mu_i^2 \bar{T}_i^*(t) = \bar{g}_i(t), \quad t > 0, \quad i = 1, 2, \ldots \tag{8a}$$

$$\bar{T}_i^*(0) = 0 \tag{8b}$$

where the transformed source term $\bar{g}_i(t)$ is given by:

$$\bar{g}_i(t) = \frac{1}{L_z}\int_0^{L_x} \tilde{\psi}_i(x)q(x,t)dx \tag{8c}$$

Once $q(x,t)$ is the function to be estimated, the integration given by Eq. (8c) must be calculated for each trial function $q(x,t)$ proposed within the inverse problem solution. In order to avoid costly numerical integrations in the iterative analysis of the inverse problem solution, a semi-analytic integration is proposed:

$$\int_0^{L_x} \tilde{\psi}_i(x)q(x,t)dx = \sum_{m=2}^{M} \int_{x_{m-1}}^{x_m} \tilde{\psi}_i(x)\hat{q}_m(x,t)dx \tag{9}$$

where $\hat{q}_m(x,t)$ are simpler representations of the source term, defined in the sub regions $[x_{m-1}, x_m]$ for which analytical integration of the eigenfunctions is still obtainable. In this work we consider the discretization of the source term in M subdomains and consider a linear representation in each sub-domain, allowing for analytical integration employing symbolic computation (Wolfram, 2005).

Even though in principle the transformed problem given by Eqs. (8a-c) allows for analytic solution, the transformed source term $\bar{g}_i(t)$ also presents unknown time variation, to be estimated within the inverse problem, and numerical integration in time would be required. Hence, the *NDSolve* routine of the Mathematica system (Wolfram, 2005) was employed to numerically handle Problem (8), yielding solutions for the transformed temperatures $\bar{T}_i^*(t)$, with $i = 1, 2, ..., N$ where N is the truncation order chosen in the inverse formula, Eq. (6b), for the desired accuracy. Finally, the inverse formula is employed, together with the filter, to yield the solution for the desired potential $T(x,t)$ at any desired position x and time instant t.

3. INVERSE PROBLEM

In this work the inverse problem was formulated in order to estimate the boundary heat flux $q(x,t)$ by using transient measurements taken at the surface in $z = L_z$, considered to be taken through an infrared thermography system, where the spatial temperatures are taken at discrete points of the surface (pixels) over a grid with center points $x_i = i\Delta x$, $i = 1, \ldots, N_i$, where N_i is the total number of measurements in the space domain with intervals by $\Delta x = L_x / N_i$. The vector of measurements can be written as:

$$\mathbf{Y}^T = \left(\vec{Y}_1 \ , \ \vec{Y}_2 \ , \ldots , \vec{Y}_{N_t} \right) \tag{10}$$

where $\vec{Y}_j \ , \ j = 1, 2, ... N_t$, contains the measured spatial temperatures at each acquisition time instant t_j. That is:

$$\vec{Y}_j \ = \left(Y_{j1} \ , \ Y_{j2} \ , \ldots , Y_{jN_i} \right) \tag{11}$$

so that a total of $D = N_i \, N_t$ measurements are available.

The sought heat flux $q(x,t)$ was discretized over a grid with $NP = NP_i \times NP_t$ nodes, yielding NP parameters to be estimated, q_{ij}, $i = 1, 2, ..., NP_i$, $j = 1, 2, ..., NP_t$, corresponding to $q_{ij} = q(x_i, t_j)$. Hence, the following vector of sought parameters can be written:

$$\mathbf{P}^T = \left[q_1, q_2, ..., q_{NP} \right] \tag{12}$$

In the present work the inverse problem is solved through the Bayesian framework (Kaipio and Sommersalo, 2004), in which the Bayes' theorem is employed to combine the new information (measurements) with the previously available information (prior). In this case, the inverse problem solution is the posterior probability density, which can be written as:

$$\pi_{posterior}(\mathbf{P}) = \pi(\mathbf{P} \,|\, \mathbf{Y}) = \frac{\pi(\mathbf{P}) \pi(\mathbf{Y} \,|\, \mathbf{P})}{\pi(\mathbf{Y})} \tag{13}$$

where $\pi_{posterior}(\mathbf{P})$ is the posterior probability density, $\pi(\mathbf{P})$ is the prior density, $\pi(\mathbf{Y} \,|\, \mathbf{P})$ is the likelihood function and $\pi(\mathbf{Y})$ is the marginal probability density of the measurements, which acts as a normalizing constant. In order to draw samples from the posterior distribution, the Metropolis-Hastings algorithm (Kaipio and Sommersalo, 2004) is employed in this work. The implementation starts with the selection of a proposal distribution $p(\mathbf{P}^*, \mathbf{P}^{(t-1)})$, which is used to draw a new candidate, $\mathbf{P}^*$, given the current state of the Markov chain, $\mathbf{P}^{(t-1)}$. Starting from an initial state $\mathbf{P}^{(0)}$, then the following steps are repeated:

1. Sample a candidate $\mathbf{P}^*$ from the proposal distribution $p(\mathbf{P}^*, \mathbf{P}^{(t-1)})$.
2. Calculate the acceptance factor:

$$R = \min \left[1, \frac{\pi(\mathbf{P}^* \,|\, \mathbf{Y}) \, p(\mathbf{P}^{(t-1)}, \mathbf{P}^*)}{\pi(\mathbf{P}^{(t-1)} \,|\, \mathbf{Y}) \, p(\mathbf{P}^*, \mathbf{P}^{(t-1)})} \right] \tag{14}$$

3. Generate a random value U sampled from a uniform distribution in the intercal [0,1].
4. If $U \leq R$, set $\mathbf{P}^{(t)} = \mathbf{P}^{*}$. Otherwise, set $\mathbf{P}^{(t)} = \mathbf{P}^{(t-1)}$.
5. Return to step 1.

Hence, a sequence of samples is generated to represent the posterior distribution and inference from this probability distribution is obtained from the samples $\left\{\mathbf{P}^{(0)}, \mathbf{P}^{(1)}, \mathbf{P}^{(2)}, ..., \mathbf{P}^{(n)}\right\}$, where the first n_b states before the equilibrium distribution is achieved must be discarded (the burn-in period).

In order to calculate the acceptance factor in the iterative procedure described above, expressions must be available for the likelihood function, $\pi(\mathbf{Y}|\mathbf{P})$, and the prior density, $\pi(\mathbf{P})$, in Eq. (13). Considering the measurement errors are additive and follow a normal distribution with zero mean and covariance matrix given by $\mathbf{W}$, the likelihood function can be written as:

$$\pi(\mathbf{Y}|\mathbf{P}) = (2\pi)^{-D/2} \left|\mathbf{W}\right|^{-1/2} \exp\left\{-\frac{1}{2}[\mathbf{Y} - \boldsymbol{\Theta}(\mathbf{P})]^T \mathbf{W}^{-1}[\mathbf{Y} - \boldsymbol{\Theta}(\mathbf{P})]\right\} \tag{15}$$

where $\boldsymbol{\Theta}(\mathbf{P})$ is the vector containing the solution of the direct (forward) problem, Eqs. (3a-i), at the same locations and time instants of the available measurements, employing the values of $\mathbf{P}$.

In order to model the prior density, besides considering a positivity constraint for the heat flux in all cases, two different Markov Random Fields priors are examined: a total variation density and a Gaussian smoothness density. The total variation prior is given in the form:

$$\pi(\mathbf{P}) \propto \exp\left[-\frac{\gamma}{2} TV(\mathbf{P})\right] \tag{16}$$

where, for the present case,

$$\begin{aligned} TV(\mathbf{P}) = \sum_{i=2}^{NP_i-1}\sum_{j=2}^{NP_t-1} \Delta t\left[\left|q(x_i,t_j) - q(x_{i+1},t_j)\right| + \left|q(x_i,t_j) - q(x_{i-1},t_j)\right|\right] + \\ \Delta x\left[\left|q(x_i,t_j) - q(x_i,t_{j+1})\right| + \left|q(x_i,t_j) - q(x_i,t_{j-1})\right|\right] \end{aligned} \tag{17}$$

The Gaussian smoothness density considered in this work can be written as:

$$\pi(\mathbf{P}) \propto \exp\left[-\frac{\alpha}{2}\sum_{j=1}^{NP_t}\left[\sum_{i=1}^{NP_i-1}\left[q(x_{i+1},t_j) - q(x_i,t_j)\right]^2\right] - \frac{\alpha}{2}\sum_{i=1}^{NP_i}\left[\sum_{j=1}^{NP_t-1}\left[q(x_i,t_{j+1}) - q(x_i,t_j)\right]^2\right]\right] \tag{18}$$

Finally, considering the combination of the total variation prior for regularization in the space domain and the Gaussian smoothness prior for regularization in the time domain, the following prior model is considered:

$$\pi(\mathbf{P}) \propto \exp\left[-\frac{\gamma}{2}\sum_{i=2}^{NP_i-1}\sum_{j=2}^{NP_t-1} \Delta t\left[\left|q(x_i,t_j) - q(x_{i+1},t_j)\right| + \left|q(x_i,t_j) - q(x_{i-1},t_j)\right|\right] - \frac{\alpha}{2}\sum_{i=1}^{NP_i}\left[\sum_{j=1}^{NP_t-1}\left[q(x_i,t_{j+1}) - q(x_i,t_j)\right]^2\right]\right] \tag{19}$$

4. RESULTS AND DISCUSSIONS

For the test case examined in this work it was considered a plate with lateral dimensions of 80x80mm and 1.5mm thickness. A material with relatively low thermal conductivity was chosen, as typical in electronic chip packaging ($k = 0.2\text{W/mK}$ and $\rho c_p = 7.2\times10^5\,\text{J/m}^3\text{K}$). The heat transfer coefficient was chosen as $h = 15\text{W/m}^2\text{K}$, typical of natural convection, with $T_\infty = 20^\circ\text{C}$. In order to present a challenging test case for the sought heat flux $q(x,t)$, it was considered a function with two abrupt transitions in space and smooth variation in time, given by Eq. (20) and illustrated in Figure 2.

$$q(x,t) = \begin{cases} 1000\left|\sin\left(\dfrac{\pi t}{3000}\right)\right|; x < 0.02; x > 0.06 \\ 0; \quad \text{elsewhere} \end{cases} \tag{20}$$

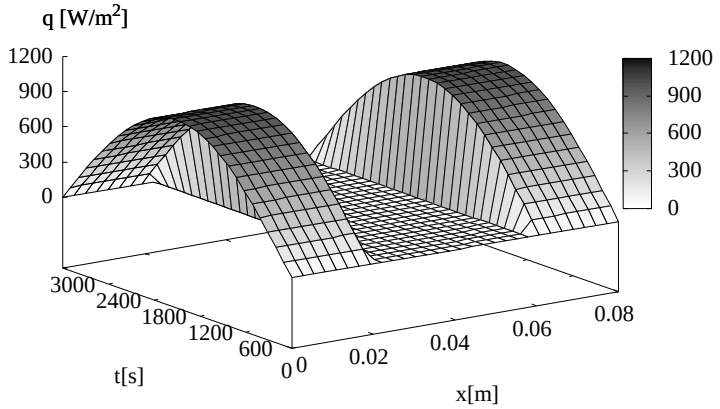

Figure 2. Test case considered, $q(x,t)$.

The sought heat flux $q(x,t)$ was discretized over a grid with 30x30 nodes, yielding *NP* = 900 parameters to be estimated, q_{ij}, $i=1,2,...,30$, $j=1,2,...,30$, corresponding to $q_{ij}=q(x_i,t_j)$. The sub-regions defined by these nodes in the space domain are employed for the semi-analytic integration, Eq. (9). For the inverse problem solution, experimental data were simulated as obtained through an infrared thermography system at the face $z=L_z$, considering 50 measurement points in space, from $x=0$ to $x=0.08\text{m}$, and 50 measurements in time, up to $t=3000s$, yielding a total of 2,500 measurements. The simulated experimental data were obtained by calculating the exact analytical solution via the Classical Integral Transform Technique (Mikhailov and Ozisik, 1984) employing the exact heat flux, Eq. (20), and adding noise with a Gaussian distribution with zero mean and $\sigma=0.7^{o}\text{C}$ standard deviation. Regarding the Markov Chain Monte Carlo method, in all cases here presented the proposal density was considered as a uniform distribution, $U[P_i^{(t-1)}-\delta, P_i^{(t-1)}+\delta]$, $i=1,2,...,NP$, with $\delta=2.5$. The length of the Markov chains was set with 100,000 states, being the first 60,000 neglected as the burn-in period, enough for the chains to converge to the equilibrium distribution.

Table 1 presents the convergence behavior of the calculated temperatures with different truncation orders (N) in the summation present in the inversion formula, Eq. (6b), at some selected positions at $t=100\text{s}$. The solution presented with truncation order N = 100 is converged to the five digits shown, demonstrating that with N = 15 the results are converged to at least three significant digits. Hence, in the inverse problem solution N = 15 was employed in all cases presented.

Table 1. Convergence behavior of the calculated temperature field at $t=100s$.

N	$x=0.01$	$x=0.02$	$x=0.03$	$x=0.04$
5	22.982	21.602	20.223	19.651
10	23.318	21.602	19.887	20.126
15	23.134	21.602	20.071	20.028
20	23.164	21.602	20.041	19.986
100	23.168	21.602	20.036	20.001

Some results are now reported for the inverse problem solution considering the three different prior models described in Section 3, i.e. Case 1: total variation prior; Case 2: Gaussian smoothness prior; and Case 3: the combination of both, with the total variation for regularization in space and the Gaussian smoothness for regularization in time. The regularization parameters were empirically chosen in the first two priors in order to yield a satisfactory regularization and the same values were repeated in the third prior model. In all cases here presented the following values were employed: $\gamma=0.0015$ and $\alpha=0.00002$. Figures 3(a,b) present the estimated heat flux, together with the exact known values, for the three prior models described above, presenting in (a) the time evolution of the flux at $x=0.01\text{m}$, and in (b) the flux distribution at $t=500\text{s}$. A first important observation is the good results obtained in all three cases, demonstrating the robustness of the Markov Chain Monte Carlo method in estimating heat fluxes with strength variation both in space and time, even in the challenging test case chosen, mixing two abrupt shifts in space and a smooth variation in time. A more careful look at these results, though, indicates that the prior model combining the total variation and the Gaussian smoothness priors, Case 3, yielded slightly better results, closer to the exact sought flux and presenting smaller variations, both in time and space.

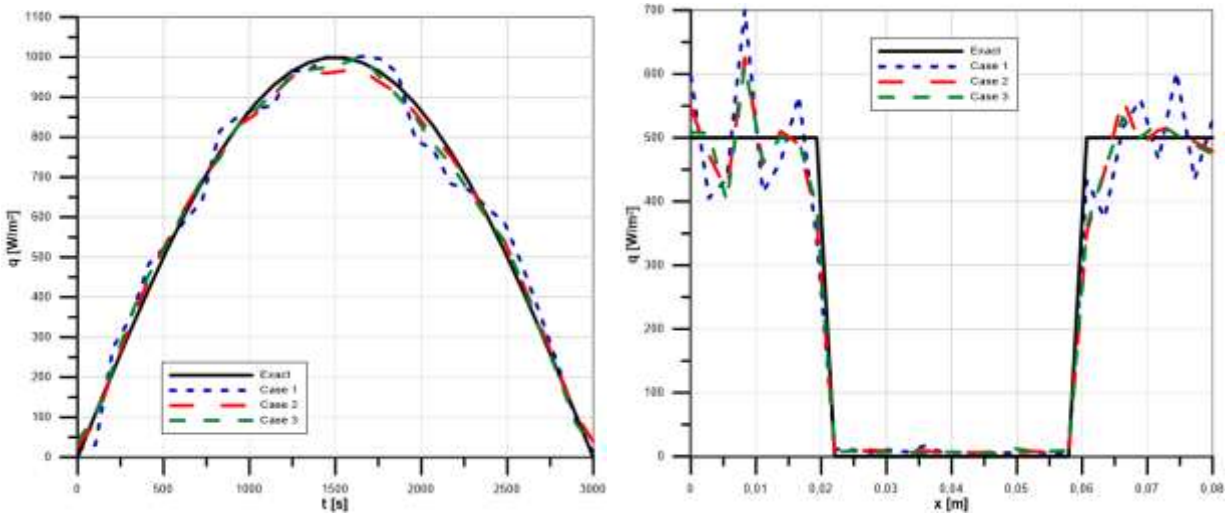

(a) (b)

Figure 3. Estimated flux: (a) $q(0.01,t)$; (b) $q(x,500)$.

In order to present a more detailed comparison regarding the estimates obtained in the three cases, Table 2 also presents the RMS error of the estimated heat flux and the estimated temperature field, as well as the estimate of the total energy applied to the plate, defined as:

$$RMS_q = \sqrt{\frac{1}{NP_i}\frac{1}{NP_j}\sum_{i=1}^{NP_i}\sum_{j=1}^{NP_j}\left[q_{ij} - q_{est,ij}\right]^2}\ ,\ RMS_T = \sqrt{\frac{1}{N_i}\frac{1}{N_j}\sum_{i=1}^{N_i}\sum_{j=1}^{N_j}\left[T_{\exp,ij} - T_{est,ij}\right]^2}\ ,\ Q = \int_0^{t_f}\int_0^{L_y}\int_0^{L_x} q_{est}(x,t)\,dx\,dy\,dt \qquad (21a\text{-}c)$$

where q_{ij} is the discretization of the exact heat flux, $q_{est,ij}$ is the discretization of the estimated heat flux, $q_{est}(x,t)$ is a first order interpolation of the discretized estimated heat flux, $T_{\exp,ij}$ are the experimental data employed, and $T_{est,ij}$ is the discretized temperature field obtained employing the estimated heat flux. Observing the values of RMS error of the estimated flux in Table 2, one confirms the impression from the results presented in Figures 3(a,b), i.e. the estimated flux using the prior model combining the total variation for regularization in space and the Gaussian smoothness for regularization in time (Case 3), presented the lowest value, whereas Case 1 presented the worst result. The same is true if one compares the RMS error of the estimated temperature field, in which Case 3, together with Case 2, yielded the temperature predictions that better fit the experimental data. Observing the estimation of the total energy applied to the plate, Case 2 presented the better estimation, with a result very similar to Case 3. It is worth noting that even in the worst result, in Case 1, the estimated energy is only 1.2% higher than the exact value. The acceptance ratio in the MCMC iterative procedure, also shown in Table 2, presents a slightly higher value for Case 3, but quite similar to the others.

Table 2. Calculated parameters of the inverse problem solution.

Parameters	Exact	Case 1	Case 2	Case 3
RMS_q [W/m^2]	0	104.38	87.12	86.78
RMS_T [°C]	0.70	0.98	0.85	0.85
Q [J]	6111.55	6186.94	6172.24	6175.71
Acc. Ratio	-	13.34%	14.34%	14.36%

Finally, Figures 4(a-c) present some more detailed results regarding the inverse problem solution with the combination of the total variation and Gaussian smoothness for the prior model. Figure 4(a) depicts the estimated flux for the whole spatial and time domain, confirming the good estimates obtained throughout. Figure 4(b) depicts the residuals between the estimated temperature field and the experimental data, showing no significant signature and small magnitudes. Figure 4(c) present the temperature profile at $t = 500$s (estimated and experimental), confirming the model predictions are well fitted to the measurements and, once more, confirming the low magnitude of the residuals and no significant signature.

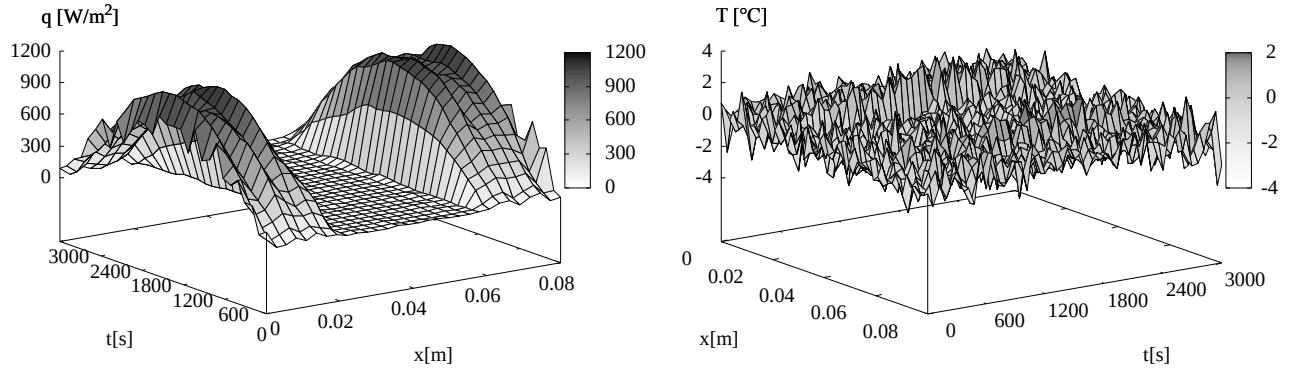

(a) (b)

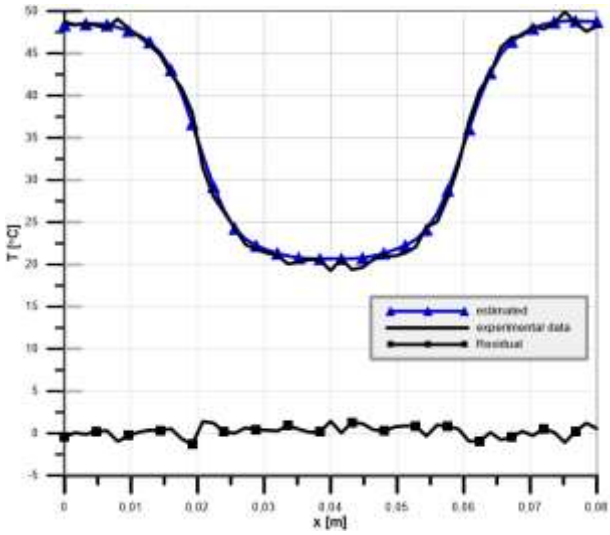

(c)

Figure 4. Results for Case 3: (a) estimated heat flux; (b) residuals; (c) estimated and experimental temperatures at $t = 500s$.

5. CONCLUSIONS

This work addressed the inverse heat conduction problem of boundary heat flux estimation, with space and time varying strengths, through non-intrusive temperature measurements, employing a combination of integral transforms for the forward problem and the Markov Chain Monte Carlo method for the inverse problem. Three cases were considered, employing different prior models derived from the Markov Random Fields theory, namely a total variation prior, a Gaussian smoothness prior and the combination of both (total variation for regularization in the space domain and Gaussian smoothness for regularization in the time domain). The results indicate the feasibility of the proposed approach, with good results obtained in all three cases, but slightly better for the third case, in which the combination of the total variation and Gaussian priors was tested. The research should now proceed towards the examination of heat fluxes with different functional forms and temperature measurements with higher experimental error.

6. REFERENCES

BarCohen, A. and Wang, P., 2012. "Thermal Management of On Chip Hot Spot". Journal of Heat Transfer, Vol. 134.

Chen, T.-C. and Hsu, S.-J., 2007. "Input Estimation Method in the Use of Electronic Device Temperature Prediction and Heat Flux Inverse Estimation". Numerical Heat Transfer, Part A: Applications: An International Journal of Computation and Methodology, Vol. 52, pp. 795–815.

Chen, W.-L. and Yang, Y.-C., 2008. "Estimation of the Transient Heat Transfer Rate at the Boundary of an Electronic Chip Packaging". Numerical Heat Transfer, Part A: Applications: An International Journal of Computation and Methodology, Vol. 54, pp. 945–961.

Cheng, J.-T. and Chen, C.-L., 2010. "Active thermal management of on-chip hot spots using EWOD-driven droplet microfluidics". Exp Fluids, Vol. 49, pp. 1349–1357.

Cotta, R. M., 1993. Integral transforms in computational heat and fluid flows. CRC Press, Florida.

Cotta, R.M. and Mikhailov, M.D., 1997. Heat Conduction: Lumped Analysis, Integral Transforms, Symbolic Computation, Wiley-Interscience, Chichester, UK.

Doudard, C., Calloch, S., Hild, F. and Roux, S., 2010. "Identification of heat source fields from infrared thermography: Determination of 'self-heating' in a dual phase steel by using a dog bone sample". Mechanics of Materials, Vol. 42, Issue 1, pp. 55–62.

Eren, G., Aubreton, O., Meriaudeau, F., Secades, L. A. S., Fofi, D., Naskali, A. T., Truchetet, F., and Ercil, A., 2009. "Scanning from heating: 3D shape estimation of transparent objects from local surface heating". Optics Express, Vol. 17, Issue 14, pp. 11457–11468.

Hastings, W., 1970. "Monte Carlo sampling methods using Markov chains and their applications". Biometrika, Vol. 57, No. 1, pp. 97–109.

Hetsroni, G., Mosyak, A. and Segal, Z., 2001. "Nonuniform Temperature Distribution in Electronic Devices Cooled by Flow in Parallel Microchannels". IEEE Transcations on Components and Packaging Technologies, Vol. 24, pp. 16–23.

Kaipio, J. and Sommersalo, E., 2004. Statistical and Computational Inverse Problems. Springer-Verlag, New York.

Knupp, D. C., Naveira-Cotta, C. P., Ayres, J. V. C., Orlande, H. R. B. and Cotta, R. M., 2012. "Space-variable thermophysical properties identification in nanocomposites via integral transforms, Bayesian inference and infrared thermography". Inverse Problems in Science and Engineering, Vol. 20, pp. 609–637.

Le Niliot, C. and Lefèvre, F., 2001. "A Method for Multiple Steady Line Heat Sources Identification in a Difusive System: Application to an Experimental 2D Problem". International Journal of Heat and Mass Transfer, Vol. 44, pp. 1425–1438.

Marinetti, S. and Valivov, V., 2010. "IR thermographic detection and characterization of hidden corrosion in metals: General analysis". Corrosion Science, Vol. 52, Issue 3, pp. 865–872.

Mikhailov, M. D. and Ozisik, M. N., 1984. Unified analysis and solutions of heat and mass diffusion. John Wiley & Sons, New York.

Mital, M., Scott, and E. P., 2006. "Thermal Detection of Embedded Tumors using Infrared Imaging". Journal of Biomechanical Engineering, Vol. 129, Issue 1, pp. 33–39.

Orlande, H. R. B., Dulikravich, G. S., Neumayer, M., Watzenig, D. and Colaço, M. J. 2014. "Accelerated Bayesian Inference for the Estimation of Spatially Varying Heat Flux in a Heat Conduction Problem". Numerical Heat Transfer, Part A: Applications: An International Journal of Computation and Methodology, Vol. 65, pp. 1–25.

Pradere, C., Joanicot, M., Batsale, J., Toutain, J. and Gourdon, C., 2006, "Processing of temperature field in chemical microreactors with infrared thermography". Quantitative InfraRed Thermography Journal, Vol. 3, Issue 1, pp. 117–135.

Silva Neto, A. J. and Osizik, M. N., 1993. "Simultaneous Estimation of Location and Timewise-Varying Strength of a Plane Heat Source". Numerical Heat Transfer, Part A: Applications: An International Journal of Computation and Methodology, Vol. 24, pp. 467–477.

Silva Neto, A. J. and Osizik, M. N., 1994. "The estimation of space and time dependent strength of a volumetric heat source in a one-dimensional plate". International Journal of Heat and Mass Transfer, Vol. 37, No. 6, pp. 909–915.

Su, J. and Silva Neto, A. J., 2001. "Two-dimensional inverse heat conduction problem of source strength estimation in cylindrical rods". Applied Mathematical Modelling, Vol. 25, pp. 861–872.

Wang, J. and Zabaras, N., 2004. "A Bayesian inference approach to the inverse heat conduction problem". International Journal of Heat and Mass Transfer. Vol. 47. pp. 3927–3941.

Wolfram, S., 2005. The Mathematica Book, Cambridge/Wolfram Media.

7. RESPONSIBILITY NOTICE

The authors are the only responsible for the printed material included in this paper.